

Journal Pre-proof

Task-dependent changes in functional connectivity during the observation of social and non-social touch interaction

Haemy Lee Masson, Ineke Pillet, Bart Boets, Hans Op de Beeck



PII: S0010-9452(19)30428-9

DOI: <https://doi.org/10.1016/j.cortex.2019.12.011>

Reference: CORTEX 2792

To appear in: *Cortex*

Received Date: 31 May 2019

Revised Date: 18 October 2019

Accepted Date: 9 December 2019

Please cite this article as: Lee Masson H, Pillet I, Boets B, Op de Beeck H, Task-dependent changes in functional connectivity during the observation of social and non-social touch interaction, *CORTEX*, <https://doi.org/10.1016/j.cortex.2019.12.011>.

This is a PDF file of an article that has undergone enhancements after acceptance, such as the addition of a cover page and metadata, and formatting for readability, but it is not yet the definitive version of record. This version will undergo additional copyediting, typesetting and review before it is published in its final form, but we are providing this version to give early visibility of the article. Please note that, during the production process, errors may be discovered which could affect the content, and all legal disclaimers that apply to the journal pertain.

© 2019 Published by Elsevier Ltd.

**Task-dependent changes in functional connectivity during the observation
of social and non-social touch interaction**

Haemy, Lee Masson^{a,b*}; Ineke, Pillet^a; Bart, Boets^b; and Hans, Op de Beeck^a

^aBrain and Cognition, KU Leuven, 3000 Leuven, Belgium

^bCenter for Developmental Psychiatry, KU Leuven, 3000 Leuven, Belgium

Correspondence should be addressed to Haemy Lee Masson, Department of Brain and Cognition, Tiensestraat 102, box 3714, 3000 Leuven, Belgium. E-mail: haemy.leemasson@kuleuven.be. Telephone: +32 16 32 32 46.

Abstract

Previous studies have identified a collection of brain areas that show neural selectivity for the distinction between human-to-human and human-to-object interactions, including regions implicated in sensory and social processing. It remains largely unknown, however, how the functional communication between these areas changes with the type of interaction. Combining a generalized psychophysiological interaction (gPPI) analysis and independent component analysis (ICA), the current study sought to identify the context-sensitive modulation of the functional network architecture during touch observation. Thirty-seven participants watched 75 video clips displaying social and non-social touch events during a functional imaging scan. A gPPI analysis of pre-defined regions of interest revealed that social-cognitive brain regions show enhanced interregional coupling during social touch observation, both among social-cognitive brain regions and between social-cognitive regions and sensory regions. Conversely, during non-social touch observation, a significantly stronger coupling among brain areas within the system that processes the unimodal sensory information was observed. At the level of large-scale brain networks extracted with ICA, stronger connectivity between 11 pairs of networks, including default mode networks, was observed during social touch observation, while only three pairs of networks showed stronger connectivity during non-social touch observation. The current study identifies the presence of context-dependent changes in functional brain architecture based on whether the touch recipient is a person or an object, highlighting an increased exchange of neural information for social processing.

Keywords

social touch observation; social cognition; functional connectivity; generalized psychophysiological interaction (gPPI) analysis; independent component analysis (ICA)

Abbreviations

FC, functional connectivity; gPPI, generalized psychophysiological interaction; IC, independent component; ICA, independent component analysis; MDL, minimum description length; PO, parietal operculum; Precu, precuneus; PCA, principal components analysis

Journal Pre-proof

1. Introduction

The sense of touch enables us to efficiently interact with both social and physical aspects of the environments. While the biological motion involved in touching behaviors in both situations may be similar, the goal and meaning of the touch are highly dependent on the touch recipient, such as whether it is a person or an object. In the former situation, we communicate emotion through touch (Hertenstein, Holmes, McCullough, & Keltner, 2009; Hertenstein, Keltner, App, Buleit, & Jaskolka, 2006), while in the latter situation we explore, recognize, and manipulate objects (Klatzky, Lederman, & Metzger, 1985). For instance, we express our emotion by stroking the arm of a loved one, while we test the texture of fabric by stroking the surface with our hands. Therefore, predicting and attributing meaning to touch may begin with identifying whether the touch is used in a social or non-social context.

The underlying neurophysiological mechanisms supporting these two contrasting functional roles of the sense of touch have been well documented, including segregated neural pathways that connect the periphery and the brain (Johansson, Trulsson, Olsson, & Westberg, 1988; Johnson, 2001; McGlone, Wessberg, & Olausson, 2014; Moehring, Halder, Seal, & Stucky, 2018; Vallbo, Olausson, Wessberg, & Norrsell, 1993).

Neuroimaging studies have also confirmed marked differences in the neural mechanisms underlying visual perception of social vs. non-social touch (Blakemore, Bristow, Bird, Frith, & Ward, 2005; Lee Masson, Van De Plas, Daniels, & Op de Beeck, 2018; Morrison, Bjornsdotter, & Olausson, 2011). In particular, the observation of social touch interactions, in contrast to non-social touch, elicits stronger neural activations and more informative multi-variate representations in the somatosensory cortex (Blakemore et al., 2005; Lee Masson et al., 2018; Morrison et al., 2011) and the brain regions implicated in social cognition, including the temporoparietal junction (TPJ) and medial prefrontal cortex (MPFC) (Lee Masson et al., 2018; Sliwa & Freiwald, 2017). In contrast, the observation of object-

oriented touch elicits relatively stronger activation in object processing areas, such as fusiform gyrus (Lee Masson et al., 2018).

To date, it remains unclear how social vs. non-social aspects of touch events dynamically reorganize the functional architecture of the brain since the aforementioned studies have focused on localizing a series of brain regions showing either increased activation or enhanced representational information in response to observed touch. However, complex cognitive functions, including social cognition, cannot be achieved by one specific brain region that processes information in isolation from other brain regions. Instead, it has long been suggested that cognition is the result of dynamic integration and coordination of the collective brain activity across several regions (Shine et al., 2019; Tononi & Edelman, 1998).

The present study sought to characterize the functional relevance of alterations in the brain network architecture during the observation of social and non-social touch by employing a multi-method approach. First, we took a theory-driven approach by first selecting brain regions of interest (ROI) thought to be involved in the processing of visually presented touch events and sought to investigate the functional communication between them. Second, to complement this theory-driven approach, we also performed a data-driven, model-free, multivariate independent component analysis (ICA) to extract the brain networks processing visually presented touch events with a blind source separation technique (Vince D. Calhoun, Liu, & Adalı, 2009; Mckeown et al., 1998). Finally, we assess context-dependent changes in regional and network level functional connectivity (FC) with a generalized psychophysiological interaction (gPPI) analysis (McLaren, Ries, Xu, & Johnson, 2012).

Interpreting the affective state of two people exchanging touch requires social cognition such as theory of mind (ToM). Numerous neuroimaging studies have shown that TPJ and MPFC are consistently activated whenever people perform all sorts of tasks requiring mental state reasoning (for review, Schurz, Radua, Aichhorn, Richlan, & Perner, 2014). In

addition to those two core social brain regions implicated in ToM, precuneus (precu), middle temporal gyrus (MTG), and superior temporal gyrus (STG) are also consistently activated during three types of ToM tasks, the false-belief task, the emotion vs. physical pain stories task, and the passive observation of a movie depicting another person's experiences (Jacoby, Bruneau, Koster-Hale, & Saxe, 2016). Based on the involvement of these brain regions in mental state reasoning and previous findings on social interaction processing (Lee Masson et al., 2018; Sliwa & Freiwald, 2017; Wurm, Caramazza, & Lingnau, 2017), we hypothesize that the functional communication among aforementioned social-cognitive brain regions/networks, implicated in ToM, would be enhanced during the observation of social touch as compared to non-social touch. Furthermore, given the involvement of the somatosensory mirror system in social touch processing (Keysers, Kaas, & Gazzola, 2010), we hypothesized that the somatosensory cortex, which is involved in self-experienced touch processing, would show increased FC with social-cognitive brain regions when subjects viewed social touch interactions. We also hypothesize enhanced functional coupling among visual brain regions/networks during the observation of non-social human-object interactions (Chao, Haxby, & Martin, 1999; Mechelli, Sartori, Orlandi, & Price, 2006).

At the network level, given that the social brain network, including the default mode network (DMN), has been resolved through data-driven ICA approach in a previous study (Mars, Neubert, et al., 2012; McCormick, van Hoorn, Cohen, & Telzer, 2018), we expect those networks to be extracted and to communicate more with other sensory networks during social touch observation.

2. Materials and Methods

2. 1. Participants

MRI scans were collected for 37 participants (28 males; mean age = 25 years, range = 19 – 38). The full dataset comprises a reanalysis geared towards FC of data that were previously

analyzed with multivariate pattern analysis (MVPA) (21 participants from Lee Masson et al., 2018, and the 16 other neurotypical participants from Lee Masson, Pillet, Amelynck, Van De Plas, Hendriks, Op de Beeck, et al., 2019). All participants had normal or corrected-to-normal vision and had no previous psychiatric nor neurological history. All participants provided written informed consent before the experiment. The study was approved by the Medical Ethical Committee of KU Leuven (S53768 and S59577). Since we analyzed existing data, the sample sizes in our analyses were identical to that of the original source studies. With respect to the secondary analyses, we report all data exclusions (if any), all inclusion/exclusion criteria, whether inclusion/exclusion criteria were established prior to secondary data analysis, all manipulations, and all measures that were included the reanalysis.

2.2. Stimuli

We used a set of stimuli created and validated in a previous study (Lee Masson & Op de Beeck, 2018). The set consists of 39 video clips displaying an interpersonal touch scene (social touch) and 36 video clips displaying a person manipulating an object (non-social touch) (Fig. 1).

Fig. 1. Example snapshots of the social and non-social stimuli. Images displaying interpersonal touch events are shown in an orange-colored box. Non-social touch events, displaying different interactions with various objects, are shown in a light blue-colored box. The complete set of video materials can be found at <https://osf.io/8j74m/>.

We intentionally matched the body movements across the social and the non-social touch scenes (e.g., hugging a person vs. carrying a box) to avoid that this variable could induce differences in the strength of FC between the two conditions. By doing so, the recipient (a person vs. an object) of the touch becomes the only element that differs between the two conditions. Details about stimulus creation and validation can be found in Lee Masson & Op de Beeck (2018). Stimuli are available online as dynamic video clips (<https://osf.io/8j74m/>).

2.3. MRI data acquisition

MRI data were obtained on a research-dedicated 3T Philips scanner with a 32-channel coil at the University Hospitals Leuven. For the functional data, whole brain images (37 axial slices with voxel size $2.7 \times 2.7 \times 3 \text{ mm}^3$ without a gap, and without fully covering cerebellum) were acquired with echo planar (EPI) T2*-weighted sequences with the following acquisition parameters: repetition time (TR) = 2000 ms, echo time (TE) = 30 ms, flip angle (FA) = 90° , field of view (FOV) = $216 \times 216 \text{ mm}$, and in-plane matrix = 80×80 . Each run comprised of 239 volumes. The T1-weighted anatomical images were acquired with a magnetization prepared rapid gradient echo (MP-RAGE) sequence, with $0.98 \times 0.98 \times 1.2 \text{ mm}^3$ resolution (182 axial slices, FOV = $250 \times 250 \text{ mm}$, TR = 9.6 ms, TE = 4.6 ms, FA = 8° , in-plane matrix = $256 \times 256 \text{ mm}$).

2.4. Visual fMRI experiment

During the scan sessions, participants watched video clips and responded whenever they detected the touch initiator wearing a sweatshirt of a pre-instructed color (black vs. grey). This task assured that participants paid attention to the video clips. This orthogonal task was designed to keep participants from falling asleep. Notably, we designed our task in this way to investigate spontaneous stimulus-related modulation of FC during the implicit processing of observed social vs. non-social touch. All the videos ($N = 75$) were presented in random order once per run in an event-related design (number of runs = 6 or 7, about 50 mins of scanning, mean number of runs = 6.4 after discarding some runs with excessive head motion). Each trial consists of a video presentation (3s) and an inter-stimulus interval (ISI, 3s) during which a participant performed the task by pressing a button. The total duration of each run took 7.8 min: 3 blocks within the run \times (baseline displaying a fixation cross for 6s + 25 trial per block \times (video presentation for 3s + 3s ISI)). To relieve the participant's fatigue, after each run, they were encouraged to take a short break in the scanner before performing the next run. Participants were able to pay attention up until the end, given that task performance of the last

run was 97.2 (the group averaged median). All the videos were projected on a screen behind the scanner and viewed through a mirror mounted on the head coil. The videos were presented and the responses were recorded by Psychophysics Toolbox Version 3.0.12 (PTB-3) (Kleiner et al., 2007) in Matlab (R2015a, The Mathworks, Natick, MA). Presentation codes are available online (<https://osf.io/hpwjx/>).

2.5. Identifying brain regions (ROIs) processing observed touch

ROIs, known to be involved in observed touch processing, were selected and defined based on the group-level results of a previous study with a combination of functional and anatomical criteria (Lee Masson et al., 2018). This includes visual (Thompson & Baccus, 2012; Vangeneugden, Peelen, Tadin, & Battelli, 2014), social (Jacoby et al., 2016), and somatosensory regions (Ebisch et al., 2008; Meyer, Kaplan, Essex, Damasio, & Damasio, 2011; Rolls et al., 2003; F. W. Smith & Goodale, 2015): Brodmann area (BA) 17, 18, 19, 37, V5, MTG, STG, TPJ, Precu, MPFC, BA3, 1, 2, and parietal operculum (PO). As such, we have 14 ROIs categorized into putative visual, social-cognition, and somatosensory networks based on the function and anatomical location of each ROI (Fig. 2). Notably, in this study, we assigned ROIs to the putative network based on their primary role reported in the literature (e.g., despite involvement of the somatosensory cortex in social processing — such as the processing of somatosensory experiences of others — BA3, 1, 2 are assigned to the somatosensory network as their primary role is to process tactile information).

Fig. 2. **A visual depiction of the selected ROIs.** The red mark in the brain image indicates the selected areas of each functionally-defined ROI. BA = Brodmann Area, MTG = Middle Temporal Gyrus, STG = Superior Temporal Gyrus, TPJ = Temporo-Parietal Junction, Precu = Precuneus, dmPFC = dorsal medial PreFrontal Cortex. PO = Parietal Operculum.

Methods to define these ROIs were exactly the same as in our previous report (Lee Masson et al., 2018). Here we again provide full details on the analysis steps implemented specifically for ROI selection. To select voxels within the most relevant anatomical boundaries, anatomical masks were obtained from various sources: the PickAtlas software

(Maldjian, Laurienti, Kraft, & Burdette, 2003) for most of the ROIs, the SPM Anatomy toolbox (Eickhoff et al., 2005) for V5 and PO (OP1 (Eickhoff, Schleicher, Zilles, & Amunts, 2006)), and the parcellation atlas (Mars, Sallet, et al., 2012) for TPJ. Within each anatomical mask, we selected the voxels that were activated by the most relevant functional contrast at the group level with the statistical threshold $P_{uncorrected} < 0.001$. Details are the following: we used both the visual fMRI experiment for ROIs belonging to either the visual network or the social-cognition network and the separate functional touch localizer run for ROIs belonging to the somatosensory network. During the separate touch localizer run, participants received rubber band snapping (at a distance of about 8cm) and brush-stroke with the velocity of 5 cm/s on the ventral surface of the right and left forearms while lying in the scanner. To fit the general linear model (GLM) to the aforementioned functional data, first, we preprocessed all functional images with the statistical parametric mapping (SPM 12) toolbox. Functional images were 1) corrected for slice timing differences, 2) re-aligned to the mean image of the first run, 3) normalized by warping them to a Montreal Neurological Institute (MNI) space with a re-sampling size of $2 \times 2 \times 2$ mm, 4) spatially smoothed using Gaussian kernels with an 8 mm full-width at half maxima (FWHM). For the first-level analysis, a standard GLM was fitted to the preprocessed functional data. All regressors of experimental conditions (social, non-social touch videos, and baseline for visual fMRI experiment and brush-stroke and rubber band snapping for a touch localizer run) were modeled as either delta functions matching the onset time of each regressor (duration = 0, an event-related design, visual fMRI experiment) or boxcar functions (duration = 10s, block design, the touch localizer run). Each function was convolved with a canonical hemodynamic response function. A temporal high-pass filter (1/128 Hz) was used. 6 Motion parameters were included in all GLMs as nuisance covariates. Brain activation evoked by all touch videos and fixation cross were contrasted for the visual fMRI experiment, and brain activation evoked by receiving touch and rest were contrasted for

the touch localizer run. Lastly, standard random-effect group-level analyses were conducted to identify significantly activated voxels in the aforementioned contrasts in the whole brain. This group activation was used to select the voxels within an anatomical mask. Table S1 illustrates statistical and spatial information about the obtained clusters for each ROI. Lastly, to ensure the independence of the BOLD signals in each ROI, we removed overlapping voxels among neighboring ROIs, similarly to our previous study (Lee Masson et al., 2018). ROIs were converted into binary masks for further analysis. This procedure is identified as step 1 in Fig. 3.

Fig. 3. A schematic figure showing an overview of the workflow (see Methods for more details). Step1: Each ROI, except somatosensory areas, was defined by selecting voxels located within the anatomical mask that showed stronger univariate activation during the observation of touch as compared to the observation of the fixation cross. The somatosensory areas were defined by selecting voxels located within the anatomical mask that showed stronger activation during actual touch stimulation as compared to rest. Notably, spheres were used for visualization purposes. Refer to Fig. 2. for the actual voxel clusters that make up each ROI. **Step2:** an ICA approach groups every voxel in the whole-brain into a functional unit, called an independent component (IC), based on the similarity of the features in BOLD time-course across voxels, yielding a group spatial map and time-course of each IC. Each group spatial map was labeled with an appropriate network descriptor based on the result of spatial correlation with the template, such as the DMN and visual network. Subsequently, temporal regression was performed to compute the degree of synchronization (reflected in ICA_{β}) between the time-course of the network and the stimulus events for each task condition, social, non-social, and baseline. In the end, the networks showing differences (reflected in F and $P-FDR$, the 4th and 5th columns in Table 2) in the degree of synchronization depending on task condition were selected to further investigate network-level connectivity. **Step3:** The average time-course was extracted and then a PPI regressor was generated for each seed region (ROI/network) by combining psychological and physiological regressors. This PPI regressor was included in the model explaining the time-course of each target region (ROI/network) to identify the strength of the functional relationship (reflected in $gPPI_{\beta}$) between a seed and a target region for each task condition. **Step4:** A paired t-test was used to determine significantly stronger FC between each pair of ROIs/networks for the contrast of social vs. non-social touch.

2.6. Identifying networks processing observed touch

2.6.1. Independent component analysis

ROI-to-ROI FC analysis may not provide a complete picture of how the entire brain networks communicate in a task-dependent manner as the selection of the ROIs depends on a priori knowledge and assumptions. To comprehensively characterize network communication in the entire brain, in addition to ROI-to-ROI FC analysis, we also adopted a data-driven multivariate approach. In particular, ICA (Vince D. Calhoun et al., 2009; McKeown et al., 1998) decomposes mixed signals in the whole brain into maximally independent components (ICs) each of which explains unique variance of fMRI data. We applied spatial ICA,

implemented in the Group ICA Toolbox (<http://mialab.mrn.org/software/>, GIFT version 3.0b), to the preprocessed fMRI data (i.e., slice-time corrected, realigned, normalized, and smoothed data using an 8mm Gaussian kernel) to identify groups of brain regions having temporally coherent BOLD signal fluctuations during the observation of touch.

First, similarly to previous studies (Cisler et al., 2013; Jarrahi et al., 2015; Thye, Ammons, Murdaugh, & Kana, 2018), the dimensions of fMRI data were reduced, and the number of ICs required to fully describe the total variance of data was estimated using a minimum description length (MDL) criterion (Li, Adalı, & Calhoun, 2007). The optimal number of ICs was estimated to be 25. Next, data reduction was performed twice at the individual and group level using standard principal components analysis (PCA), followed by an independent component estimation using the Infomax ICA algorithm (Bell & Sejnowski, 1995). The Infomax ICA was repeated ten times using the ICASSO toolbox implemented in GIFT to extract the most stable 25 ICs at the group level. According to the results of an estimated quality index from the ICASSO, which ranges from 0 to 1 (values approaching 1 imply reliable extraction of the component; values approaching 0 imply a randomly produced, unreliable component), all 25 ICs were reliable (quality index values > 0.9). To compute the individual participant's ICs, we performed GICA back-reconstruction on the group ICs using parameters of PCA compression and projection (Calhoun, Adalı, Pearlson, & Pekar, 2001). Resulting spatial images and time-courses were converted to z-scores. Here, the resulting z-score of each voxel reflects its contribution to the time-course of each IC. Individuals' back reconstructed, and then z-score converted ICs were then used to compute a group mean spatial map and a group mean time-course of each IC.

2.6.2. Identifying the task-relevant networks from ICs

The analysis pipeline mentioned below is illustrated in step 2 of Fig. 3.

Spatial components: Following previous studies (Xu et al., 2013; Zhang & Li, 2012), we performed spatial sorting, implemented in GIFT, to discard noise-related ICs. We computed the spatial correlation between a group-level spatial t-map of each IC (thresholded at z -score > 3) and probabilistic maps of the grey matter (GM), white matter (WM), and cerebrospinal fluid (CSF) provided with SPM12. The voxels that make up each IC should be predominantly located in the GM. Accordingly, the ICs whose group-level spatial map contain a large number of voxels located in WM and CSF, most likely represent physiological noise. Among the 25 ICs, 7 ICs which either related to CSF (coefficient of determination (r^2) > 0.05) or did not relate to GM ($r^2 < 0.001$) were removed. None of the ICs were spatially correlated with WM. Based on visual inspection, two additional ICs consisting of voxels located in the cerebellum ($N = 1$) or around the edges of the brain ($N = 1$) were additionally excluded from further analysis. We excluded ICs composed of the cerebellum because the cerebellum was not completely covered during the scan due to the short TR. Using the same methods, we labeled the remaining 16 ICs with functional or regional descriptors (e.g., DMN or visual network). In particular, each IC was correlated with the Resting State Networks templates (S. M. Smith et al., 2009) available in GIFT, and the label of the template with the maximal correlation value was assigned to the IC. From this point forward, we will refer to the ICs as “networks” and we will designate particular ICs/networks by referring to its label (e.g., DMN).

Temporal components: Similarly to how we functionally defined ROIs, rather than selecting all 16 networks, we first verified whether BOLD signal fluctuations of each network respond differently to task and baseline conditions. To do this we assessed task-related modulation over time-courses of the remaining 16 networks using the temporal sorting feature implemented in GIFT (for a similar approach, see Assaf et al., 2009; Jarrahi et al., 2015; Ye et al., 2012).

The temporal sorting function performs a multiple regression analysis to find the association between BOLD signal fluctuations of each network and the reference time-courses of the three regressors (i.e., social touch, non-social touch, and baseline condition displaying a fixation cross), and measures the degree to which the onset of stimulus presentation modulates the time-course of each network during the task and baseline. Consequently, for each individual, a set of 16 beta coefficients (ICA_{β}) is obtained for each of the three task regressors, which indicate to what extent the task regressor is associated with a particular network. Next, a group-level mean ICA_{β} -value is computed to indicate to what extent the time-course of each network is engaged during the social, non-social, and baseline conditions at the group level.

For each network, a within-subjects ANOVA was performed to determine the main effect of conditions on the ICA_{β} -values (the false discovery rate (FDR)-corrected for type-1 errors). Afterward, using a one sample t-test, group-level spatial maps of each network that showed task-related engagement were thresholded at $P_{FWE} < 0.001$ and converted into binary maps for further analysis.

2.7. Functional Connectivity Analyses

2.7.1. Pre-processing

With the SPM 12 toolbox the following preprocessing steps were carried out: (1) functional images were corrected for slice timing differences; (2) realigned to the mean image of the first run; (3) the anatomical image was co-registered to functional images; (4) segmented to GM, WM, and cerebrospinal fluid; and then (5) the functional images and segmented GM, WM, and CSF images were normalized to the MNI template with the voxels resliced to $2 \times 2 \times 2$. We did not smooth the images (Alakörkkö, Saarimäki, Glerean, Saramäki, & Korhonen, 2017). The subsequent procedures were performed with the CONN (CONN 17) toolbox (Whitfield-Gabrieli & Nieto-Castanon, 2012).

Prior to the first-level estimation of FC, we removed the artifacts from the fMRI data using the component-based noise correction method (CompCor), as implemented in the CONN toolbox. Specifically, we estimated outlying volumes based on the motion (subject-motion threshold = 0.9 mm) and global signal (z -value threshold = 5) deviations using an Artifact Detection and Repair toolbox, as implemented in the CONN toolbox. This variable was used for scrubbing during the de-noising step. This de-noising step also includes regressing out: (1) 10 principal components of the WM and CSF signal from the data calculated with PCA; (2) head motion-related artifacts by using six head motion parameters and their first derivatives; and (3) task-related BOLD signals by performing linear de-trending. Bandpass-filtering was performed to remove slowly fluctuating signal (0.008 Hz) such as scanner drift.

2.7.2. Generalized psychophysiological interaction analyses

We examined how brain regions interact in a task-dependent manner, using a gPPI analysis implemented in CONN toolbox (McLaren et al., 2012). PPI analysis is a type of task-based FC analysis that identifies voxels/ROIs of which the BOLD response time course (change in neural activity over time) is more related to that of a seed region in a given psychological context. Unlike the standard PPI analysis that includes contrast information when forming a psychological regressor, the gPPI approach convolves the BOLD signal with the canonical hemodynamic response function for each condition before making the contrast, forming a separate psychological regressor for each condition. This approach has been known to improve the fit of the regression model for event-related fMRI data (McLaren et al., 2012).

The following description is shown in step 3 of Fig. 3. First, we extracted an averaged BOLD time-course across selected voxels for each ROI/network and used it as a physiological regressor. For a subject-level analysis, we generated a PPI regressor for each condition by calculating the element-by-element product between psychological and physiological

regressors. Second, we computed how strongly the time-course of one ROI/network is correlated with the PPI regressor of another. Unlike correlational analysis, gPPI is based on multiple regression, thereby generating different β values when the seed and target regions are reversed. This pair-wise computation was made for every possible pair-wise combination of selected ROIs/networks to measure task-dependent changes in FC for each participant. Third, results were converted to z-scores using the Fisher's z-transformation before calculating a group-level averaged FC. We conducted a random-effects analysis across participants to measure the differences in FC between social and non-social conditions at the group-level. Statistical inferences were made using a one-sample paired t-test comparing ROI/network connectivity for the social vs. non-social condition. We corrected for the rate of type1 errors with the FDR at the analysis-level (the number of tests performed; that is, each possible pair combination of ROIs/network) instead of the ROI/network-level (the number of ROIs/networks selected).

All the data necessary to replicate the results of this study are contained in Open Science Framework (<https://osf.io/hpwjx/>).

3. Results

3.1. Task-dependent changes in ROI-to-ROI connectivity

We sought to examine changes in FC among the key brain regions involved in processing visually presented touch events, i.e., brain areas that are part of the visual, somatosensory, or social-cognitive brain networks. The results of the gPPI analysis demonstrated that task-dependent changes in inter-regional functional coupling among ROIs did indeed take place, as a function of whether participants watched human-human or human-object interactions.

Overall, as illustrated in Fig. 4 (red vs. blue lines) and Table 1 (orange vs. sky-blue at the 5th column), enhanced connectivity strength among ROI-pairs was more extensively found during the observation of social touch compared to non-social touch (number of ROI-pairs

showing increased FC strength during social touch observation = 23; during non-social touch observation = 7, the 5th column of Table 1). This finding is consistent with our previous study demonstrating stronger neural activation in a wide range of brain areas during the observation of social touch compared to non-social touch (Lee Masson et al., 2018).

Table 1. Detailed statistical results of the ROI-to-ROI FC for the contrast of social > non-social touch observation. The color of the cells in the first and second columns illustrate to which network each ROI theoretically belongs: the visual network is colored in green, the social-cognition network in pink, and the somatosensory network in red. The 5th column indicates whether the FC is increased during the observation of social (in orange) or non-social touch (in sky-blue). B = FC among ROIs belonging to different networks, i.e., between-networks, W = FC among ROIs belonging to the same network, i.e., within-networks

Seed	Target	T Statistics	P-FDR	FC
BA17	TPJ	4.11	0.004	Social (B)
	STG	3.09	0.031	Social (B)
BA18	BA19	-3.62	0.001	Non (W)
	TPJ	2.94	0.006	Social (B)
BA19				
BA37	STG	5.86	0.000	Social (B)
	TPJ	5.55	0.000	Social (B)
	MTG	4.15	0.004	Social (B)
	V5	3.27	0.023	Social (W)
V5	STG	4.25	0.003	Social (B)
	BA19	-3.93	0.005	Non (W)
	BA37	-3.27	0.023	Non (W)
	MTG	3.07	0.031	Social (B)
MTG	STG	6.02	0.000	Social (W)
	BA19	-5.96	0.000	Non (B)
	TPJ	4.92	0.001	Social (W)
	BA37	-4.04	0.004	Non (B)
	PO	-2.98	0.036	Non (B)
STG	MTG	3.89	0.000	Social (W)
	V5	3.05	0.004	Social (B)
TPJ	MTG	5.36	0.000	Social (W)
	STG	5.02	0.000	Social (W)
	BA17	3.75	0.008	Social (B)
	BA37	3.11	0.031	Social (B)
Precu	STG	4.04	0.004	Social (W)
	TPJ	3.20	0.026	Social (W)
	MTG	2.91	0.041	Social (W)
MPFG				
BA3				
BA1	BA18	2.83	0.045	Social (B)
BA2	STG	3.12	0.031	Social (B)
	Precu	2.87	0.043	Social (B)
PO	BA2	3.47	0.015	Non (W)

Fig. 4. Differences in the ROI-to-ROI FC for the social vs. non-social touch contrast. Illustrated are pairs of regions that demonstrated increased connectivity for the observation of social touch relative to non-social touch (red lines) and increased connectivity for non-social touch (blue lines). The color of the line connecting the two ROIs and the square box next to each ROI represents the ROI-to-ROI connectivity value, reflected in the t-value. The red mark in the brain image indicates the location of each ROI. T = t value from a one sample paired t-test, P FDR corrected < 0.05

More specifically, as hypothesized, watching a social touch scene, in contrast to a non-social touch scene, induces enhanced functional coupling between ROIs within the social-cognition system (e.g., increased FC among MTG, STG, TPJ, and Precu; Fig. 4 and Table 1). Given that mentalizing the states of others (i.e., emotional states of a touch initiator and a recipient in this context) is a core part of social cognition, we expected to observe this increased connectivity among the social brain areas during social touch observation.

The increase of the strength in FC occurred not only between social brain areas but also between social brain areas and other areas processing more basic sensory information. In particular, enhanced connectivity strength was observed between the social brain areas and the brain areas that process visual information (e.g., TPJ was strongly connected to BA17, BA18, and BA37; STG was strongly connected to BA17, BA37, and V5) or somatosensory information (STG and Precu were strongly connected to BA2).

Conversely, in the case of non-social touch scenes displaying human-object interactions, our results revealed significantly greater connectivity between ROI-pairs within the same sensory networks: enhanced functional couplings between ROIs within the visual (e.g., BA18 and V5 more strongly connected to BA19) or somatosensory networks (i.e., PO more strongly connected to BA2).

MTG, sensitive to moving human body and tool stimuli (Beauchamp, Lee, Haxby, & Martin, 2003), showed extensive task-dependent alterations in functional relationships with other brain regions. Specifically, social touch observation evoked significantly greater connectivity between MTG and other social brain areas while non-social observation evoked significantly greater connectivity between MTG and other sensory areas. For example, MTG is more strongly connected to high-level visual (BA19 and BA37) and somatosensory areas (PO). Detailed statistical information for these results is provided in Table 1.

3.2. Identifying the task-relevant networks and characterizing connectivity

3.2.1 The task-relevant networks revealed by a data-driven multivariate ICA approach

Prior to evaluating task-dependent changes in network-to-network connectivity, we first extracted networks using a data-driven multivariate ICA on the whole-brain fMRI data, which resulted in 25 networks. Among these, 8 networks were found to be related to noise and one network was located in the cerebellum. The remaining 16 networks were labeled, and as hypothesized, this ICA approach yielded four DMNs and 12 other networks comprising one visual, two sensorimotor, two precuneus, two executive control, one auditory, one language, and one salience network, as well as an unlabeled network consisting of the bilateral anterior temporal lobe, and another unlabeled network consisting of the bilateral insular cortex (Component description, Table 2). As mentioned in the method section 2.6.2, we selected the networks based on whether the degree of temporal network synchronization with the task, represented by ICA β -values, varied across task conditions.

Table 2. **Detailed statistical results of the within-subjects ANOVA on the ICA β -values (driven from the temporal sorting procedure) of social, non-social, and baseline conditions.** Additionally, the labels for each component are listed next to the component number, and the correlation (R) values between the selected template providing the label and the group spatial map of each component were also listed. N = network.

Component number	Component description	R -value	F Statistics	P -FDR
IC1	Ventral DMN (N1)	0.26/0.18	3.97	0.027
IC2	Visual Network (N2)	0.17	167.82	0.000
IC3	Sensorimotor Network (N3)	0.21	8.70	0.000
IC4	Precuneus Network (N4)	0.25	7.25	0.002
IC5	Right Executive Control Network	0.20	1.97	0.17
IC6	Auditory Network (N5)	0.27	11.73	0.000
IC7	Left Executive Control Network	0.19	1.16	0.32
IC8	Dorsal DMN (N6)	0.38	7.63	0.001
IC9	Sensorimotor Network (N7)	0.24	26.70	0.000
IC10	Noise			
IC11	Noise			
IC12	Dorsal DMN (N8)	0.26	83.39	0.000
IC13	Noise			
IC14	Dorsal DMN (N9)	0.29/0.18	25.70	0.000
IC15	Precuneus Network (N10)	0.25	101.21	0.000
IC16	Noise			
IC17	Noise			
IC18	Language Network (N11)	0.18	42.44	0.000
IC19	Noise			
IC20	Anterior Salience Network (N12)	0.20	13.32	0.000
IC21	No label found, bilateral anterior temporal lobe		1.74	0.19
IC22	Noise			
IC23	Noise			
IC24	No label found (N13), bilateral insula		4.83	0.01
IC25	Cerebellum	0.23		

According to the results of a within-subjects ANOVA test, 13 of the 16 networks showed a significant effect of task (i.e., social, non-social, and baseline) on the degree of synchronization between time-course fluctuations of the network and the task events (the last column in Table 2). According to post hoc t-tests, these task effects are mainly driven by the contrast with the baseline condition. By taking the temporal sorting approach, task-related networks could be functionally defined in the same manner as the functional ROIs (i.e., touch > baseline). The networks that differentially synchronize with the task conditions included four DMNs, two sensorimotor, two precuneus, a visual, an auditory, a language, a salience, and an unlabeled network consisting mainly of the bilateral insular cortex. Fig. 5 illustrates the group spatial maps of these 13 networks. Table S2 contains descriptions of the implicated brain regions and the list of peak MNI coordinates of these networks.

Fig. 5. **Visualization of 13 networks with their labels.** The red mark in the brain image displays voxels relevant to each network revealed by an ICA approach. These networks were included for further gPPI analysis.

3.2.2. Task-dependent changes in network-to-network connectivity

A model-free multivariate ICA approach permitted us to extract 13 networks whose degree of synchronization with the task event was differentially determined by task condition. To complement the results of the ROI-to-ROI connectivity analysis, we examined the task-dependent changes in connectivity among these 13 identified networks (Fig. 5). At the network level, ICA-gPPI results revealed enhanced functional coupling in 11 pairs of networks (red lines in Fig. 6 and Table 3) during the observation of social touch as compared to non-social touch. Three DMNs (N1, 6 and 9) showed enhanced functional coupling with other networks during the observation of social touch, suggesting that these networks share significantly much more social information with other networks than non-social information.

Table 3 **Detailed statistical results of the network-to-network FC for the contrast of social > non-social touch observation.** The 5th column indicates whether the strength of FC is increased during the observation of social or non-social touch. The visual network is colored in green, the DMN in pink, and the somatosensory network in red.

Seed	Target	T Statistics	P-FDR	FC
N1 (DMN)	N11 (Language)	3.03	0.04	Social

N2 (Visual)				
N3 (Sensorimotor)	N4 (Precu)	3.09	0.04	Social
N4 (Precu)	N5 (Auditory)	3.41	0.03	Social
	N2 (Visual)	-3.24	0.03	Non
N5 (Auditory)	N4 (Precu)	3.99	0.01	Social
	N9 (DMN)	3.08	0.04	Social
	N7 (Sensorimotor)	-3.05	0.04	Non
N6 (DMN)	N5 (Auditory)	3.41	0.03	Social
N7 (Sensorimotor)	N9 (DMN)	3.25	0.03	Social
N8 (DMN)				
N9 (DMN)	N5 (Auditory)	4.88	0.003	Social
	N11 (Language)	4.17	0.01	Social
	N13 (No Label, insula)	3.35	0.03	Social
N10 (Precu)	N4 (Precu)	4.03	0.01	Social
N11 (Language)	N9 (DMN)	3.52	0.03	Social
	N3 (Sensorimotor)	-3.31	0.03	Non
N12 (Salience)	N4 (Precu)	3.41	0.03	Social
	N11 (Language)	3.11	0.04	Social
N13 (No Label, insula)	N9 (DMN)	2.95	0.046	Social

Fig. 6. **Differences in FC between each pair of networks for the social vs. non-social touch contrast.** Illustrated are pairs of networks that demonstrated increased strength of connectivity for the observation of social touch relative to non-social touch (red lines) and increased strength of connectivity for non-social touch (blue lines). The color of the line connecting the networks and the square box next to each network represents the connectivity value, reflected in the t-value. DMN = default mode network, Precu = Precuneus, N = network, T = t value from a one sample t-test, $P_{FDR\ corrected} < 0.05$

For the opposite contrast, only three pairs of networks (blue lines in Fig. 6) showed increased connectivity. No DMN networks were part of these pairs showing stronger FC during the observation of non-social touch. The statistical details are provided in Table 3.

4. Discussion

The present study investigated the functional relevance of alterations in the brain network architecture during the observation of social (human-to-human) and non-social (human-to-object) interactions. Adapting both theory- and data-driven approaches, we were able to characterize how two different types of task — understanding the meaning of human-to-human interaction vs. human-to-object manipulation — modulate the neural functional architecture both at the level of individual brain regions and at the large-scale network level.

4.1. Increased connectivity within the social cognitive system during human-to-human social touch observation

With a hypothesis-driven, ROI-based analysis, we found increased connectivity within a set of brain areas previously identified as the social-cognitive system active during the

observation of social touch relative to non-social touch. These results extend the findings of our previous MPVA study investigating neural representations underlying the understanding of others' social touch interactions, revealing the importance of communication between biological motion selective areas (MTG and STG) and perceived valence selective areas (TPJ and Precu) (Lee Masson et al., 2018).

The role of the temporal and parietal cortex in social perception and cognition has been extensively documented, including its involvement in biological motion perception (Allison, Puce, & McCarthy, 2000), action understanding (Deen, Koldewyn, Kanwisher, & Saxe, 2015; Pelphrey, Morris, & McCarthy, 2004), and inferring mental states of others (Ciaramidaro et al., 2007; Jacoby et al., 2016; Saxe & Kanwisher, 2003). Nevertheless, task-induced changes in their functional relationships have only recently begun to be explored (McCormick et al., 2018). Our finding of increased interregional communication within the social-cognitive system during social touch observation extends previous research that showed strong functional relationships among social brain regions, including STS, TPJ, Precu, during a social evaluation task (McCormick et al., 2018).

Previous studies investigating the neural basis of social understanding of others have consistently reported strong activation in MPFC during tasks requiring inferring other's emotions and intentions, self-other distinctions, or judging other's behavior (W. Li, Mai, & Liu, 2014; Lieberman, 2007; Van Overwalle, 2009). However, similar to our previous MVPA findings that did not reveal neural selectivity for socio-affective characteristics of observed touch in the MPFC (Lee Masson et al., 2018), we did not observe increased functional communication of MPFC with other brain regions during social touch observation.

To provide a complete picture of how the entire brain networks communicate in a task-dependent manner and to complement the results revealed by the ROI-based approach, we extracted 13 task-related networks using a data-driven ICA method. Among them, four

networks were identified as the DMN. According to review studies (W. Li et al., 2014; Mars, Neubert, et al., 2012), key nodes of the DMN mainly include the medial posterior cortex, MPFC, and TPJ. Similarly, two DMNs identified in the current study include the MPFC, whereas the other two DMNs mainly cover the medial posterior cortex (Table S2). The network-level connectivity analysis revealed increased functional connections between the DMN (N6), consisting of Precu and the MPFC, and the auditory network (N5) during social touch observation. Despite its label, the auditory network includes brain regions involved in social (i.e., Precu) and emotional (insula) processing (Fig. 5). Except for one aforementioned functional connection of DMN (N6), the current study does not provide evidence of increased communication of MPFC during social touch observation. As discussed in our previous MPVA study (Lee Masson et al., 2018), performing an orthogonal task requiring color identification of the shirt of the touch initiator may not require the extensive involvement of the MPFC, which is specialized in more elaborative, effortful social processing (W. Li et al., 2014).

Two other DMNs, mainly consisting of voxels located in the medial posterior cortex, showed increased functional couplings with another network (i.e., Language Network) containing voxels located in the STG. The current study demonstrates that a data-driven ICA method can be used to cluster a collection of brain regions that make up the DMNs during the passive touch observation. Similar to ROI-based FC analysis, we observed that DMNs communicate with other networks containing social brain areas during social information processing.

4.2. Increased connectivity between the social cognitive system and the sensory system during human-to-human social touch observation

Observing social touch increases interactions between the social cognitive system and other basic sensory systems, both at the level of brain regions and large-scale networks. Firstly, the

social-cognitive system (STG, and TPJ) communicates more with areas involved both in low- (BA17 and 18) and high-level visual processing (BA37 and V5). A possible interpretation of these results is that the social and visual systems work in concert to extract socially relevant information from visually presented bodily movements of the two interacting people shown in the social touch scene.

Secondly, enhanced functional coupling with the social cognitive system (STG and Precu) was observed in the somatosensory area (BA2), a key node of the somatosensory mirror system (Keysers & Gazzola, 2009; Keysers et al., 2010). Likewise, the ICA approach revealed increased connectivity between the DMN (N9) and the sensorimotor network (N7) consisting of the bilateral postcentral gyrus.

The ability to map another person's somatosensory experience to the self, quantified by the level of neural activation in the somatosensory area, has been related to ToM and empathy mechanisms (Giummarra et al., 2015; Peled-Avron, Levy-Gigi, Richter-Levin, Korem, & Shamay-Tsoory, 2016; Schaefer, Heinze, & Rotte, 2012). In a similar vein, the somatosensory cortex, activated when receiving actual touch, has been found to exhibit neural selectivity for the perceived socio-affective meaning of observed touch (Lee Masson et al., 2018). Furthermore, perturbing this area by means of brain stimulation decreases an individual's prosocial behavior (Gallo et al., 2018). Given this converging evidence of the crucial role of the somatosensory system in higher-level social processing, enhanced communication between the social cognitive and somatosensory systems during social touch observation can be interpreted as facilitating our ability to understand other people's emotional states by directly mapping bodily experiences of others to the self. Our findings are also in line with previous studies demonstrating functional communication between nodes in the mirroring and the mentalizing systems when representing observed actions as socio-emotional expressions (Spunt & Lieberman, 2012).

Finally, in addition to the DMNs, we were able to characterize FC patterns across different networks using a data-driven ICA approach. As indicated in the results section, we observed much more communication between networks implicated in different cognitive functions during social touch observation. In particular, we observed both the salience network (N12) and the network (N13) composed of the insula showing increased connectivity with other networks. Given the role of the insula in socio-emotional processing (Uddin, 2016), this increase implies enhanced integration of visually presented social touch information with internal emotional representations. With the same gPPI method, a previous study has demonstrated increased FC between the insula and the anterior cingulate cortex (ACC), which compose the salience network, when touching a human hand (social touch) as compared to touching a mannequin hand (non-social touch) (Scalabrini et al., 2019). These findings suggest that the salience network may function as a domain-general neural system processing social touch information in cooperation with other networks.

4.3. Increased connectivity within the same sensory systems during human-to-object non-social touch observation

Visual scenes depicting object manipulation elicited more interregional communication between areas located in the same sensory system (FC between BA 18 and BA 19 in the visual system; FC of BA19 and BA37 with V5 in the visual system; and FC between BA 2 and PO in the somatosensory system). Given the role of the visual cortex in recognizing a manipulable object, these findings are very likely driven by the presence of inanimate objects in the non-social touch condition scene (Chao et al., 1999; Haxby et al., 1991). Likewise, the increased connectivity between BA2 and PO, which are part of the somatosensory system, can be explained by considering that both brain regions play a crucial role in tactile object recognition (Reed, Shoham, & Halgren, 2004) and both brain regions show increased neural activation while observing human hands engaged in object manipulation (Meyer et al., 2011).

4.4. Converging evidence from ROI-based and ICA-based measures of the context-sensitive modulation of the connectivity

In general, the results obtained using both methods showed similar context-sensitive modulation of the functional network architecture during the touch observation. Specifically, both revealed that functional couplings between brain regions and between networks occurred more strongly during the social touch observation as compared to non-social touch. Taking both approaches, we have observed converging evidence for increased communication between the brain regions/networks, implicated in social processing, and other sensory areas/networks. Our findings imply that the processing of human-to-human social interactions may be facilitated through larger-scale brain communication.

Notably, some discrepancies were observed between the results derived from both methodologies. For example, unlike an ROI-based FC approach (null results discussed in supplementary materials), ICA-based measures of FC revealed context-dependent changes in functional communication between the salient networks, mainly consisting of the insula, and other networks (e.g., DMN). Similar discrepancies were observed between the two methodologies for the connectivity of the network, containing MPFC, with another network. Based on our findings, these two approaches appear to be complementary. The ROI approach provides information about connectivity between individual brain regions. The ICA-based FC approach seems to help find additional evidence at the network level that could not be found with the ROI-based approach. Thus, the ICA-based FC approach may be a useful tool for comprehensively characterizing network communication in the entire brain while offering the benefits of blind source separation and dimensionality reduction. Our findings are consistent with the previous study showing high similarities (though not identical) between the connectivity maps obtained during the visuo-motor task using two methodologies (Joel, Caffo, Van Zijl, & Pekar, 2011).

4.5. How our findings relate to understanding others

Social perception, action recognition, and the theory of mind are representative examples of social information processing (Yang, Rosenblau, Keifer, & Pelphrey, 2015). These social cognitive abilities enable us to understand another person's emotions, intentions, and mental states based on behavioral cues expressed during social interactions such as facial expressions, body gestures, and reciprocal touch. The present study has demonstrated that understanding others who are engaging in reciprocal touch is achieved through the engagement of various neural systems and the enhanced communication between them. Importantly, our study provides evidence that during the observation of other people's touch actions, extensive changes occur in the functional structure of the brain, depending on whether the recipient is a person or an object. Our findings suggest that the flexibility in context-dependent modulation of brain communication may be the underlying neural mechanism of social cognitive ability that enables us to understand others.

4.6. Limitations and directions for future research

In this study, we adopted both a theory-driven ROI-based and data-driven ICA-based approach. As described in the Materials and Methods section, ROI selection was already made when designing our previous multivariate pattern analysis study (Lee Masson et al., 2018). The advantage of selecting the same ROIs is that it facilitates comparisons among our publications using the same experimental design analyzed with different neuroimaging methods. Moreover, a hypothesis-driven ROI approach increases the study's sensitivity and reduces the problems of multiple comparisons. Disadvantages of the ROI approach, such as missing out some brain regions, are remediated by the data-driven multivariate ICA-based approach. However, although the ICA approach offers the benefits of dimensionality reduction and blind source separation, increasing the study's sensitivity, this approach may not

fully replace a whole brain-level ROI analysis. Thus, future studies could consider different types of FC analysis, such as whole-brain ROIs and seed-based FC analysis.

The current study raises further questions that will require future research. The directionality of the information flow remains to be investigated using a neuroimaging method with a finer temporal resolution to clarify whether the interaction is the results of top-down or bottom-up modulation. It is also necessary to clarify how connectivity patterns change over time in order to understand a dynamic structure of neural model supporting social touch perception. For example, implementing a Granger causality approach to data obtained with magnetoencephalography (MEG) can aid in answering these questions.

5. Conclusion

The present study provides novel and rich evidence that the observation of human-to-human social touch interactions, relative to non-social touch, elicits much more information exchange among key brain regions and networks. Furthermore, our findings support and extend an existing integrative neural model of social cognition (Bohl & van den Bos, 2012; Yang et al., 2015) by characterizing how strongly the somatosensory mirror network is connected to regions and networks implicated in social cognition and social perception. Lastly, the current study emphasizes the advantages of a task-based connectivity approach in revealing the context-sensitive modulation in neural functional architecture, which cannot be answered by a task-free resting state approach.

Conflict of interest

The authors have no conflict of interest to report.

Acknowledgments

The authors would like to thank Dr. Jeyoung Jung for discussion of functional connectivity analysis. We would like to also thank Dr. J. Brendan Ritchie for reading our manuscript and pointing out grammatical and vocabulary errors. This work was supported by the Marguerite-

Marie Delacroix foundation granted to Haemy Lee Masson (grant number GV/B-336), the Research Foundation Flanders (grant number G088216N) and Excellence of Science program (grant numbers G0E8718N; HUMVISCAT) granted to Bart Boets and Hans Op de Beeck, and a Hercules Grant (grant number ZW11_10) to Hans Op de Beeck.

Pre- registration statement

No part of the study procedures was pre-registered prior to the research being conducted. No part of the study analyses was pre-registered prior to the research being conducted.

CRedit authorship contribution statement

Haemy Lee Masson: Conceptualization; Data curation; Formal analysis; Funding acquisition; Investigation; Methodology; Project administration; Resources; Software; Validation; Visualization; Roles/Writing - original draft; and Writing - review & editing. **Ineke Pillet:** Investigation; and Writing - review & editing. **Bart Boets:** Funding acquisition; and Writing – Review & Editing. **Hans Op de Beeck:** Conceptualization; Funding acquisition; Resources; Supervision; and Writing - review & editing.

References

- Alakörkkö, T., Saarimäki, H., Glerean, E., Saramäki, J., & Korhonen, O. (2017). Effects of spatial smoothing on functional brain networks. *European Journal of Neuroscience*, *46*(9), 2471–2480. <https://doi.org/10.1111/ejn.13717>
- Allison, T., Puce, A., & McCarthy, G. (2000, July 1). Social perception from visual cues: Role of the STS region. *Trends in Cognitive Sciences*. Elsevier Current Trends. [https://doi.org/10.1016/S1364-6613\(00\)01501-1](https://doi.org/10.1016/S1364-6613(00)01501-1)
- Assaf, M., Jagannathan, K., Calhoun, V., Kraut, M., Hart, J., & Pearlson, G. (2009). Temporal sequence of hemispheric network activation during semantic processing: A functional network connectivity analysis. *Brain and Cognition*, *70*(2), 238–246. <https://doi.org/10.1016/j.bandc.2009.02.007>
- Beauchamp, M. S., Lee, K. E., Haxby, J. V., & Martin, A. (2003). fMRI Responses to Video and

- Point-Light Displays of Moving Humans and Manipulable Objects. *Journal of Cognitive Neuroscience*, 15(7), 991–1001. <https://doi.org/10.1162/089892903770007380>
- Bell, A. J., & Sejnowski, T. J. (1995). An information-maximization approach to blind separation and blind deconvolution. *Neural Computation*, 7(6), 1129–1159. Retrieved from <http://www.ncbi.nlm.nih.gov/pubmed/7584893>
- Blakemore, S. J., Bristow, D., Bird, G., Frith, C., & Ward, J. (2005). Somatosensory activations during the observation of touch and a case of vision-touch synaesthesia. *Brain*, 128(7), 1571–1583. <https://doi.org/10.1093/brain/awh500>
- Bohl, V., & van den Bos, W. (2012). Toward an integrative account of social cognition: marrying theory of mind and interactionism to study the interplay of Type 1 and Type 2 processes. *Frontiers in Human Neuroscience*, 6, 274. <https://doi.org/10.3389/fnhum.2012.00274>
- Calhoun, V.D., Adali, T., Pearlson, G. D., & Pekar, J. J. (2001). A method for making group inferences from functional MRI data using independent component analysis. *Human Brain Mapping*, 14(3), 140–151. <https://doi.org/10.1002/hbm.1048>
- Calhoun, Vince D., Liu, J., & Adali, T. (2009). A review of group ICA for fMRI data and ICA for joint inference of imaging, genetic, and ERP data. *NeuroImage*, 45(1), S163–S172. <https://doi.org/10.1016/J.NEUROIMAGE.2008.10.057>
- Chao, L. L., Haxby, J. V., & Martin, A. (1999). Attribute-based neural substrates in temporal cortex for perceiving and knowing about objects. *Nature Neuroscience*, 2(10), 913–919. <https://doi.org/10.1038/13217>
- Ciaramidaro, A., Adenzato, M., Enrici, I., Erk, S., Pia, L., Bara, B. G., & Walter, H. (2007). The intentional network: How the brain reads varieties of intentions. *Neuropsychologia*, 45(13), 3105–3113. <https://doi.org/10.1016/j.neuropsychologia.2007.05.011>
- Cisler, J. M., Elton, A., Kennedy, A. P., Young, J., Smitherman, S., Andrew James, G., & Kilts, C. D. (2013). Altered functional connectivity of the insular cortex across prefrontal networks in cocaine addiction. *Psychiatry Research - Neuroimaging*, 213(1), 39–46. <https://doi.org/10.1016/j.psychresns.2013.02.007>
- Deen, B., Koldewyn, K., Kanwisher, N., & Saxe, R. (2015). Functional organization of social

- perception and cognition in the superior temporal sulcus. *Cerebral Cortex*, 25(11), 4596–4609.
<https://doi.org/10.1093/cercor/bhv111>
- Ebisch, S. J. H., Perrucci, M. G., Ferretti, A., Del Gratta, C., Romani, G. L., & Gallese, V. (2008). The Sense of Touch: Embodied Simulation in a Visuotactile Mirroring Mechanism for Observed Animate or Inanimate Touch. *Journal of Cognitive Neuroscience*, 20(9), 1611–1623.
<https://doi.org/10.1162/jocn.2008.20111>
- Eickhoff, S. B., Schleicher, A., Zilles, K., & Amunts, K. (2006). The human parietal operculum. I. Cytoarchitectonic mapping of subdivisions. *Cerebral Cortex*, 16(2), 254–267.
<https://doi.org/10.1093/cercor/bhi105>
- Eickhoff, S. B., Stephan, K. E., Mohlberg, H., Grefkes, C., Fink, G. R., Amunts, K., & Zilles, K. (2005). A new SPM toolbox for combining probabilistic cytoarchitectonic maps and functional imaging data. *NeuroImage*, 25(4), 1325–1335. <https://doi.org/10.1016/j.neuroimage.2004.12.034>
- Gallo, S., Paracampo, R., Müller-Pinzler, L., Severo, M., Blömer, L., Henschel, A., ... Gazzola, V. (2018). The role of the somatosensory cortex in prosocial behavior. *ELife*, 7, e32740.
<https://doi.org/10.7554/eLife.32740>
- Giummarra, M. J., Fitzgibbon, B. M., Georgiou-Karistianis, N., Beukelman, M., Verdejo-Garcia, A., Blumberg, Z., ... Gibson, S. J. (2015). Affective, sensory and empathic sharing of another's pain: The Empathy for Pain Scale. *European Journal of Pain*, 19(6), 807–816.
<https://doi.org/10.1002/ejp.607>
- Haxby, J. V., Grady, C. L., Horwitz, B., Ungerleider, L. G., Mishkin, M., Carson, R. E., ... Rapoport, S. I. (1991). Dissociation of object and spatial visual processing pathways in human extrastriate cortex. *Proceedings of the National Academy of Sciences of the United States of America*, 88(5), 1621–1625. <https://doi.org/10.1073/pnas.88.5.1621>
- Hertenstein, M. J., Holmes, R., McCullough, M., & Keltner, D. (2009). The Communication of Emotion via Touch. *Emotion*, 9(4), 566–573. <https://doi.org/10.1037/a0016108>
- Hertenstein, M. J., Keltner, D., App, B., Bulleit, B. A., & Jaskolka, A. R. (2006). Touch communicates distinct emotions. *Emotion*, 6(3), 528–533. <https://doi.org/10.1037/1528-3542.6.3.528>
- Jacoby, N., Bruneau, E., Koster-Hale, J., & Saxe, R. (2016). Localizing Pain Matrix and Theory of

- Mind networks with both verbal and non-verbal stimuli. *NeuroImage*, 126, 39–48.
<https://doi.org/10.1016/j.neuroimage.2015.11.025>
- Jarrahi, B., Mantini, D., Balsters, J. H., Michels, L., Kessler, T. M., Mehnert, U., & Kollias, S. S. (2015). Differential functional brain network connectivity during visceral interoception as revealed by independent component analysis of fMRI time-series. *Human Brain Mapping*, 36(11), 4438–4468. <https://doi.org/10.1002/hbm.22929>
- Joel, S. E., Caffo, B. S., Van Zijl, P. C. M., & Pekar, J. J. (2011). On the relationship between seed-based and ICA-based measures of functional connectivity. *Magnetic Resonance in Medicine*, 66(3), 644–657.
- Johansson, R. S., Trulsson, M., Olsson, K. a, & Westberg, K.-G. (1988). Mechanoreceptor activity from the human face and oral mucosa. *Experimental Brain Research*, 72(FEBRUARY), 204–208.
<https://doi.org/10.1007/BF00248518>
- Johnson, K. O. (2001, August 1). The roles and functions of cutaneous mechanoreceptors. *Current Opinion in Neurobiology*. Elsevier Current Trends. [https://doi.org/10.1016/S0959-4388\(00\)00234-8](https://doi.org/10.1016/S0959-4388(00)00234-8)
- Keysers, C., & Gazzola, V. (2009). Expanding the mirror: vicarious activity for actions, emotions, and sensations. *Current Opinion in Neurobiology*, 19(6), 666–671.
<https://doi.org/10.1016/j.conb.2009.10.006>
- Keysers, C., Kaas, J. H., & Gazzola, V. (2010). Somatosensation in social perception. *Nature Reviews Neuroscience*, 11(10), 726–726. <https://doi.org/10.1038/nrn2919>
- Klatzky, R. L., Lederman, S. J., & Metzger, V. A. (1985). Identifying objects by touch: An “expert system.” *Perception & Psychophysics*, 37(4), 299–302. <https://doi.org/10.3758/BF03211351>
- Kleiner, M., Brainard, D. H., Pelli, D. G., Broussard, C., Wolf, T., & Niehorster, D. (2007). What’s new in Psychtoolbox-3? *Perception*, 36, S14. <https://doi.org/10.1068/v070821>
- Lee Masson, H., & Op de Beeck, H. (2018). Socio-affective touch expression database. *PLOS ONE*, 13(1), e0190921. <https://doi.org/10.1371/journal.pone.0190921>
- Lee Masson, H., Pillet, I., Amelynck, S., Van De Plas, S., Hendriks, M., Op de Beeck, H., & Boets, B. (2019). Intact neural representations of affective meaning of touch but lack of embodied

- resonance in autism: a multi-voxel pattern analysis study. *Molecular Autism*, 10(1), 39.
<https://doi.org/10.1186/s13229-019-0294-0>
- Lee Masson, H., Van De Plas, S., Daniels, N., & Op de Beeck, H. (2018). The multidimensional representational space of observed socio-affective touch experiences. *NeuroImage*, 175, 297–314.
<https://doi.org/10.1016/j.neuroimage.2018.04.007>
- Li, W., Mai, X., & Liu, C. (2014). The default mode network and social understanding of others: what do brain connectivity studies tell us. *Frontiers in Human Neuroscience*, 8, 74.
<https://doi.org/10.3389/fnhum.2014.00074>
- Li, Y.-O., Adalı, T., & Calhoun, V. D. (2007). Estimating the number of independent components for functional magnetic resonance imaging data. *Human Brain Mapping*, 28(11), 1251–1266.
<https://doi.org/10.1002/hbm.20359>
- Lieberman, M. D. (2007). Social Cognitive Neuroscience: A Review of Core Processes. *Annual Review of Psychology*, 58(1), 259–289. <https://doi.org/10.1146/annurev.psych.58.110405.085654>
- Maldjian, J. A., Laurienti, P. J., Kraft, R. A., & Burdette, J. H. (2003). An automated method for neuroanatomic and cytoarchitectonic atlas-based interrogation of fMRI data sets. *NeuroImage*, 19(3), 1233–1239. [https://doi.org/10.1016/S1053-8119\(03\)00169-1](https://doi.org/10.1016/S1053-8119(03)00169-1)
- Mars, R. B., Neubert, F.-X., Noonan, M. P., Sallet, J., Toni, I., & Rushworth, M. F. S. (2012). On the relationship between the “default mode network” and the “social brain.” *Frontiers in Human Neuroscience*, 6, 189. <https://doi.org/10.3389/fnhum.2012.00189>
- Mars, R. B., Sallet, J., Schüffelgen, U., Jbabdi, S., Toni, I., & Rushworth, M. F. S. (2012). Connectivity-based subdivisions of the human right “temporoparietal junction area”: Evidence for different areas participating in different cortical networks. *Cerebral Cortex*, 22(8), 1894–1903. <https://doi.org/10.1093/cercor/bhr268>
- McCormick, E. M., van Hoorn, J., Cohen, J. R., & Telzer, E. H. (2018). Functional connectivity in the social brain across childhood and adolescence. *Social Cognitive and Affective Neuroscience*, 13(8), 819–830. <https://doi.org/10.1093/scan/nsy064>
- McGlone, F., Wessberg, J., & Olausson, H. (2014). Discriminative and Affective Touch: Sensing and Feeling. *Neuron*, 82(4), 737–755. <https://doi.org/10.1016/j.neuron.2014.05.001>

- Mckeown, M. J., Makeig, S., Brown, G. G., Jung, T.-P., Kindermann, S. S., Bell, A. J., & Sejnowski, T. J. (1998). Analysis of fMRI data by blind separation into independent spatial components. *Human Brain Mapping, 6*(3), 160–188. [https://doi.org/10.1002/\(SICI\)1097-0193\(1998\)6:3<160::AID-HBM5>3.0.CO;2-1](https://doi.org/10.1002/(SICI)1097-0193(1998)6:3<160::AID-HBM5>3.0.CO;2-1)
- McLaren, D. G., Ries, M. L., Xu, G., & Johnson, S. C. (2012). A generalized form of context-dependent psychophysiological interactions (gPPI): A comparison to standard approaches. *NeuroImage, 61*(4), 1277–1286. <https://doi.org/10.1016/j.neuroimage.2012.03.068>
- Mechelli, A., Sartori, G., Orlandi, P., & Price, C. J. (2006). Semantic relevance explains category effects in medial fusiform gyri. *NeuroImage, 30*(3), 992–1002. <https://doi.org/10.1016/j.neuroimage.2005.10.017>
- Meyer, K., Kaplan, J. T., Essex, R., Damasio, H., & Damasio, A. (2011). Seeing touch is correlated with content-specific activity in primary somatosensory cortex. *Cerebral Cortex, 21*(9), 2113–2121. <https://doi.org/10.1093/cercor/bhq289>
- Moehring, F., Halder, P., Seal, R. P., & Stucky, C. L. (2018). Uncovering the Cells and Circuits of Touch in Normal and Pathological Settings. *Neuron, 100*(2), 349–360. <https://doi.org/10.1016/J.NEURON.2018.10.019>
- Morrison, I., Bjornsdotter, M., & Olausson, H. (2011). Vicarious Responses to Social Touch in Posterior Insular Cortex Are Tuned to Pleasant Caressing Speeds. *Journal of Neuroscience, 31*(26), 9554–9562. <https://doi.org/10.1523/JNEUROSCI.0397-11.2011>
- Peled-Avron, L., Levy-Gigi, E., Richter-Levin, G., Korem, N., & Shamay-Tsoory, S. G. (2016). The role of empathy in the neural responses to observed human social touch. *Cognitive, Affective, & Behavioral Neuroscience, 16*(5), 802–813. <https://doi.org/10.3758/s13415-016-0432-5>
- Pelphrey, K. A., Morris, J. P., & McCarthy, G. (2004). Grasping the intentions of others: The perceived intentionality of an action influences activity in the superior temporal sulcus during social perception. *Journal of Cognitive Neuroscience, 16*(10), 1706–1716. <https://doi.org/10.1162/0898929042947900>
- Reed, C. L., Shoham, S., & Halgren, E. (2004). Neural Substrates of Tactile Object Recognition: An fMRI Study. *Human Brain Mapping, 21*(4), 236–246. <https://doi.org/10.1002/hbm.10162>

- Rolls, E. T., O'Doherty, J., Kringelbach, M. L., Francis, S., Bowtell, R., & McGlone, F. (2003). Representations of pleasant and painful touch in the human orbitofrontal and cingulate cortices. *Cerebral Cortex*, *13*(3), 308–317. <https://doi.org/10.1093/cercor/13.3.308>
- Saxe, R., & Kanwisher, N. (2003). People thinking about thinking people: The role of the temporoparietal junction in “theory of mind.” *NeuroImage*, *19*(4), 1835–1842. [https://doi.org/10.1016/S1053-8119\(03\)00230-1](https://doi.org/10.1016/S1053-8119(03)00230-1)
- Scalabrini, A., Ebisch, S. J. H., Huang, Z., Di Plinio, S., Perrucci, M. G., Romani, G. L., ... Northoff, G. (2019). Spontaneous Brain Activity Predicts Task-Evoked Activity During Animate Versus Inanimate Touch. *Cerebral Cortex*. <https://doi.org/10.1093/cercor/bhy340>
- Schaefer, M., Heinze, H. J., & Rotte, M. (2012). Embodied empathy for tactile events: Interindividual differences and vicarious somatosensory responses during touch observation. *NeuroImage*, *60*(2), 952–957. <https://doi.org/10.1016/j.neuroimage.2012.01.112>
- Schurz, M., Radua, J., Aichhorn, M., Richlan, F., & Perner, J. (2014, May 1). Fractionating theory of mind: A meta-analysis of functional brain imaging studies. *Neuroscience and Biobehavioral Reviews*. Pergamon. <https://doi.org/10.1016/j.neubiorev.2014.01.009>
- Shine, J. M., Breakspear, M., Bell, P. T., Ehgoetz Martens, K., Shine, R., Koyejo, O., ... Poldrack, R. A. (2019). Human cognition involves the dynamic integration of neural activity and neuromodulatory systems. *Nature Neuroscience*, *22*(2), 289–296. <https://doi.org/10.1038/s41593-018-0312-0>
- Sliwa, J., & Freiwald, W. A. (2017). A dedicated network for social interaction processing in the primate brain. *Science*, *356*(6339), 745–749. <https://doi.org/10.1126/science.aam6383>
- Smith, F. W., & Goodale, M. A. (2015). Decoding visual object categories in early somatosensory cortex. *Cerebral Cortex*, *25*(4), 1020–1031. <https://doi.org/10.1093/cercor/bht292>
- Smith, S. M., Fox, P. T., Miller, K. L., Glahn, D. C., Fox, P. M., Mackay, C. E., ... Beckmann, C. F. (2009). Correspondence of the brain's functional architecture during activation and rest. *Proceedings of the National Academy of Sciences*, *106*(31), 13040–13045. <https://doi.org/10.1073/pnas.0905267106>
- Spunt, R. P., & Lieberman, M. D. (2012). An integrative model of the neural systems supporting the

- comprehension of observed emotional behavior. *NeuroImage*, 59(3), 3050–3059.
<https://doi.org/10.1016/J.NEUROIMAGE.2011.10.005>
- Thompson, J. C., & Baccus, W. (2012). Form and motion make independent contributions to the response to biological motion in occipitotemporal cortex. *NeuroImage*, 59(1), 625–634.
<https://doi.org/10.1016/j.neuroimage.2011.07.051>
- Thye, M. D., Ammons, C. J., Murdaugh, D. L., & Kana, R. K. (2018). Differential recruitment of theory of mind brain network across three tasks: An independent component analysis. *Behavioural Brain Research*, 347, 385–393. <https://doi.org/10.1016/j.bbr.2018.03.041>
- Tononi, G., & Edelman, G. M. (1998). Consciousness and Complexity. *Science*, 282(5395), 1846–1851.
- Uddin, L. Q. (2016, January 19). Salience processing and insular cortical function and dysfunction. *Nature Reviews Neuroscience*. Nature Publishing Group. <https://doi.org/10.1038/nrn3857>
- Vallbo, A., Olausson, H., Wessberg, J., & Norrsell, U. (1993). A system of unmyelinated afferents for innocuous mechanoreception in the human skin. *Brain Research*, 628(1–2), 301–304. Retrieved from <http://www.ncbi.nlm.nih.gov/pubmed/8313159>
- Van Overwalle, F. (2009, March 1). Social cognition and the brain: A meta-analysis. *Human Brain Mapping*. John Wiley & Sons, Ltd. <https://doi.org/10.1002/hbm.20547>
- Vangeneugden, J., Peelen, M. V., Tadin, D., & Battelli, L. (2014). Distinct Neural Mechanisms for Body Form and Body Motion Discriminations. *Journal of Neuroscience*, 34(2), 574–585.
<https://doi.org/10.1523/JNEUROSCI.4032-13.2014>
- Whitfield-Gabrieli, S., & Nieto-Castanon, A. (2012). Conn: a functional connectivity toolbox for correlated and anticorrelated brain networks. *Brain Connectivity*, 2(3), 125–141.
- Wurm, M. F., Caramazza, A., & Lingnau, A. (2017). Action Categories in Lateral Occipitotemporal Cortex Are Organized Along Sociality and Transitivity. *The Journal of Neuroscience*, 37(3), 562–575. <https://doi.org/10.1523/JNEUROSCI.1717-16.2017>
- Xu, J., Zhang, S., Calhoun, V. D., Monterosso, J., Li, C. S. R., Worhunsky, P. D., ... Potenza, M. N. (2013). Task-related concurrent but opposite modulations of overlapping functional networks as revealed by spatial ICA. *NeuroImage*, 79, 62–71.

<https://doi.org/10.1016/j.neuroimage.2013.04.038>

Yang, D. Y.-J., Rosenblau, G., Keifer, C., & Pelphrey, K. A. (2015, April 1). An integrative neural model of social perception, action observation, and theory of mind. *Neuroscience and*

Biobehavioral Reviews. Pergamon. <https://doi.org/10.1016/j.neubiorev.2015.01.020>

Ye, Z., Kutas, M., St. George, M., Sereno, M. I., Ling, F., & Münte, T. F. (2012). Rearranging the world: Neural network supporting the processing of temporal connectives. *NeuroImage*, *59*(4),

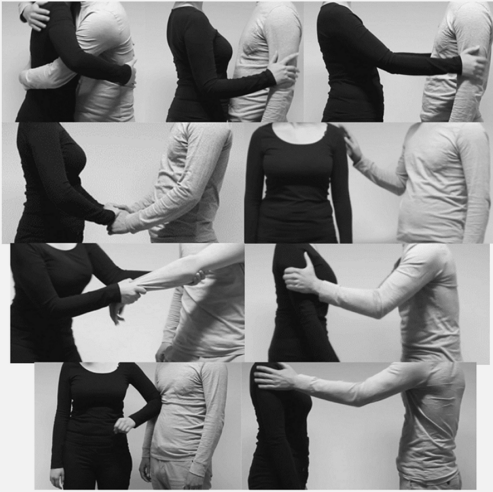
3662–3667. <https://doi.org/10.1016/J.NEUROIMAGE.2011.11.039>

Zhang, S., & Li, C. S. R. (2012). Functional networks for cognitive control in a stop signal task:

Independent component analysis. *Human Brain Mapping*, *33*(1), 89–104.

<https://doi.org/10.1002/hbm.21197>

Social (human-to-human) touch

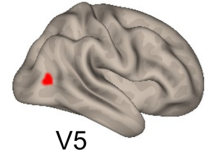
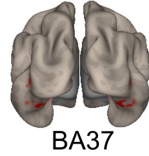
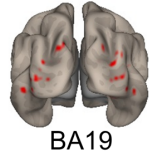
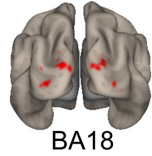
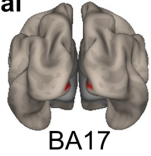


Non-social (human-to-object) touch

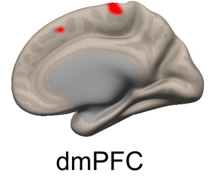
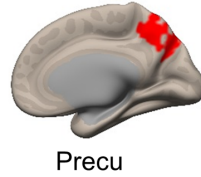
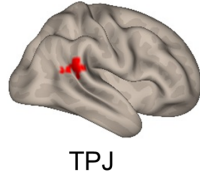
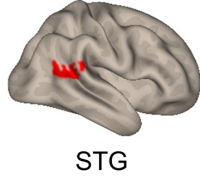
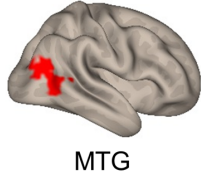


Journal Pre-proof

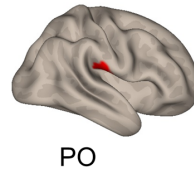
Visual



Social Cognition

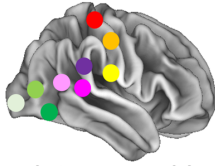


Somatosensory



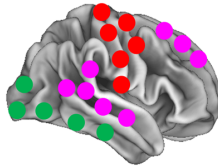
Journal Pre-proof

1. Task-relevant [observed touch] regions



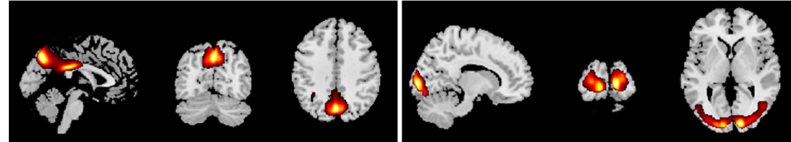
- 1) Univariate second-level GLM approach
- 2) Contrast: observed touch > baseline or actual touch > rest

2. Task-relevant [observed touch] networks

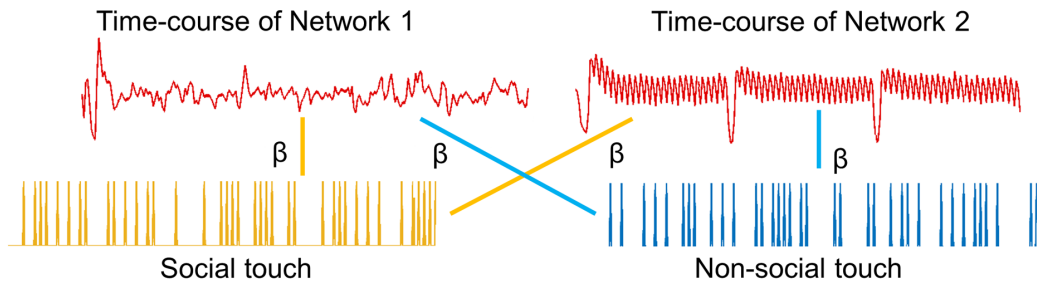


IC 1, DMN

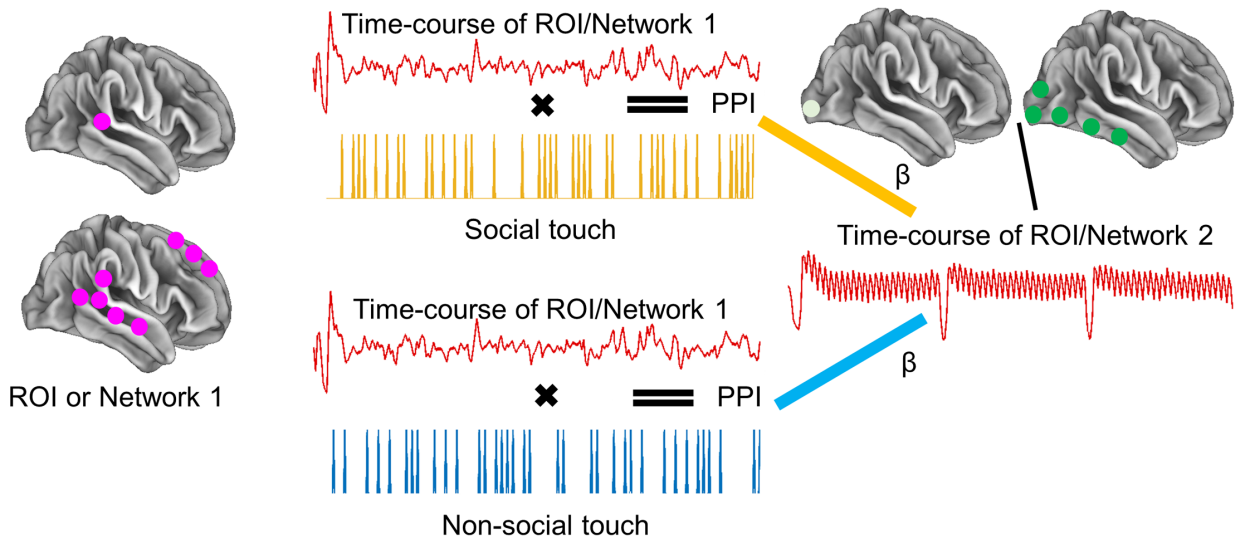
IC 2, Visual network



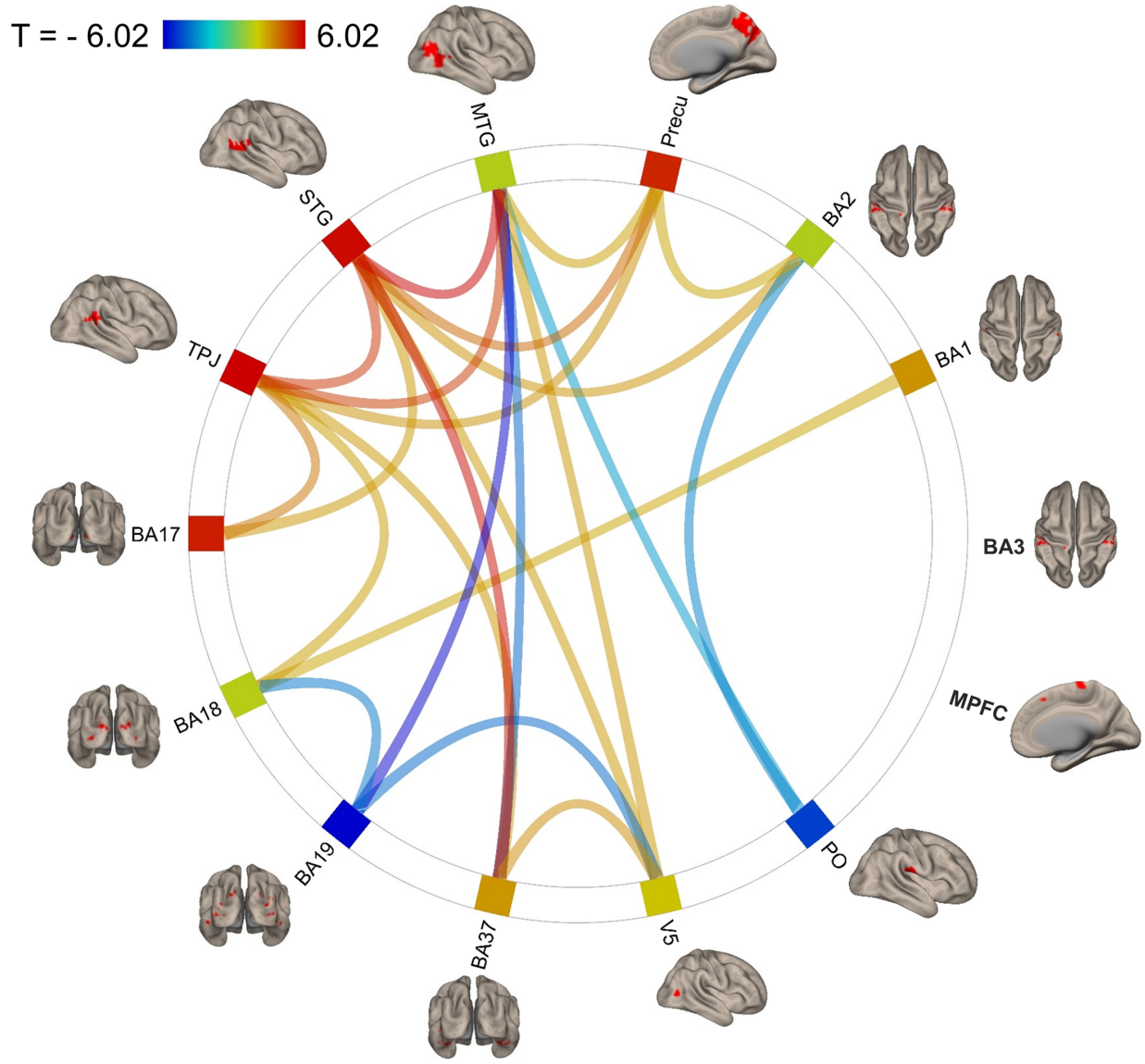
- 1) Multivariate second-level ICA approach
- 2) Spatial correlation (ICA)
- 3) Temporal regression (ICA)

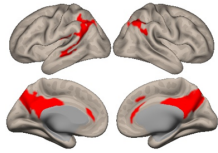


3. Task-based functional connectivity with gPPI

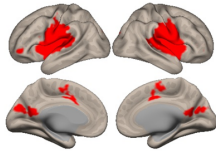


4. T-statistics on the strength of ROI- and Network-level FC (β) for the contrast of social > non-social touch

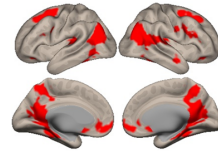




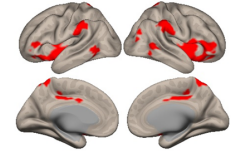
Network 1 (DMN)



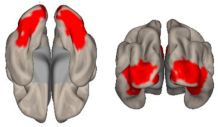
Network 5 (Auditory)



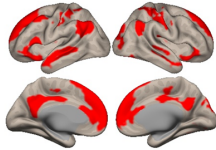
Network 9 (DMN)



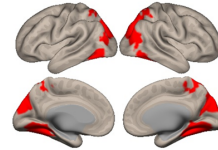
Network 13 (Insula)



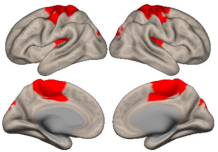
Network 2 (Visual)



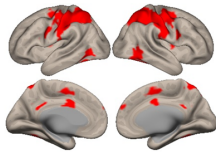
Network 6 (DMN)



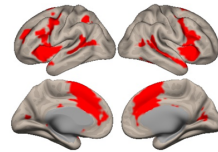
Network 10 (Precu)



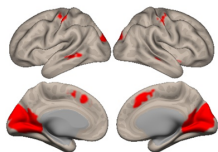
Network 3 (Sensorimotor)



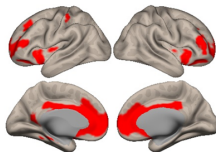
Network 7 (Sensorimotor)



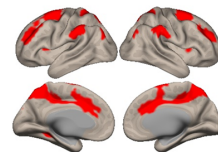
Network 11 (Language)



Network 4 (Precu)



Network 8 (DMN)



Network 12 (Salience)

Journal Pre-proof

T = - 4.88  4.88